Remote Sensing of Fire Severity: Assessing the Performance of the Normalized Burn Ratio

David P. Roy, Luigi Boschetti, and Simon N. Trigg

***Abstract*—Several studies have used satellite data to map different levels of fire severity present within burned areas. Increasingly, fire severity has been estimated using a spectral index called the normalized burn ratio (NBR). This letter assesses the performance of the NBR against ideal requirements of a spectral index designed to measure fire severity. According to index theory, the NBR would be optimal for quantifying fire severity if the trajectory in spectral feature space caused by different levels of severity occurred perpendicular to the NBR isolines. We assess how well NBR meets this condition using reflectance data sensed before and shortly after fires in the South African savanna, Australian savanna, Russian Federation boreal forest, and South American tropical forest. Although previous studies report high correlation between fire severity measured in the field- and satellite-derived NBR, our results do not provide evidence that the performance of the NBR is optimal in describing fire severity shortly after fire occurrence. Spectral displacements due to burning occur in numerous directions relative to the NBR index isolines, suggesting that the NBR may not be primarily and consistently sensitive to fire severity. Findings suggest that the development of the next generation of methods to estimate fire severity remotely should incorporate knowledge of how fires of different severity displace the position of prefire vegetation in multispectral space.**

***Index Terms*—Fire severity, remote sensing, spectral index.**

I. Introduction

WITHIN the field of the remote sensing of fire, the detection of burned areas is relatively well established [1]. A further refinement is to measure how a fire's effects vary within burned areas. Information on within-burn variability is useful to ecologists and resource managers who want to understand fire's effects on ecosystem processes, for example, vegetation recovery and succession, and to plan postfire rehabilitation and remediation. Such within-burn information may be estimated by visual examination of burned site conditions or by labor-intensive field measurements [2], [3].

One qualitative indicator used to assess fire effects within burned areas is named fire severity. Definitions of fire severity vary but are used to relate how fire changes ecosystems differentially or result in different biological responses [2], [4], [5]–[10]. Definitions also vary in terms of the amount of time elapsed before fire severity is assessed; this time can vary from one day to several years postfire (the longer time delays are necessary if the biological effects of fire are of interest).

Parameters used to estimate severity in the field include the condition and color of the soil, amount of fuel consumed, resprouting from burned plants, blackening or scorching of trees, depth of burn in the soil, and changes in fuel moisture. Although several of these parameters may not be amenable directly to optical wavelength remote sensing, or may not be related in a linear way to reflectance, field-based measures of fire severity have been used to parameterize and assess fire severity maps created using optical wavelength satellite data [2], [9]–[11].

Fire severity has been estimated remotely using spectral indices; both using single-date and multitemporal index data [6]–[12]. One index presented as a reliable means to map fire severity is called the normalized burn ratio (NBR), computed as the difference between near-infrared (NIR) and middle-infrared (MIR) reflectance divided by their sum [2].

Fire severity mapped in the field has been found to correlate with fire severity mapped using NBR, leading to suggestions that NBR provides a transferable means to measure fire severity [9]–[11]; however, there are four main grounds for caution. The first is that relatively few studies have assessed NBR-derived maps of fire severity in terms of their accuracy; furthermore, those studies that have done so, typically report relatively low overall accuracies in the range of 53% to 81% [7], [10], [11]. The second is that the formulation of the NBR was originally proposed as an index to detect burned areas rather than to evaluate them [13]; since detection and evaluation of a given target constitute fundamentally different objectives, a spectral index designed to do one of these tasks may perform poorly on the other [14]. The third more general concern is that the NBR was not designed, nor has it been assessed, in terms of relevant theory of spectral index design [14]; it is, therefore, unclear how well the wavelengths chosen, or the normalized NBR formulation, conform to the theoretical requirements for designing an index to measure fire severity. Finally, we note that as fire severity is a qualitative parameter that cannot unambiguously be defined or measured in the field, statistical correlations between field and satellite NBR-derived fire severity estimates may be indicative of several factors other than fire severity [15].

In this letter, we critically consider the prospects for using the NBR to measure severity shortly after fire occurrence. The assessment uses data collected at different sites and at different

Manuscript received June 22, 2005; revised August 12, 2005. This work was supported in part by the National Aeronautics and Space Administration (NASA) Land Cover and Land Use Change and Applications Programs under Grant NAG511251 and in part by the NASA Earth System Science Program under Grant NNG04HZ18C.

D. P. Roy is with the Geographic Information Science Center of Excellence, South Dakota State University, Brookings, SD 57007 USA (e-mail: david.roy@sdstate.edu).

L. Boschetti and S. N. Trigg are with the Department of Geography, University of Maryland, College Park, MD 20742 USA (e-mail: luigi.boschetti@hermes.geog.umd.edu; trigg@umd.edu).

Digital Object Identifier 10.1109/LGRS.2005.858485

1545-598X/$20.00 © 2006 IEEE

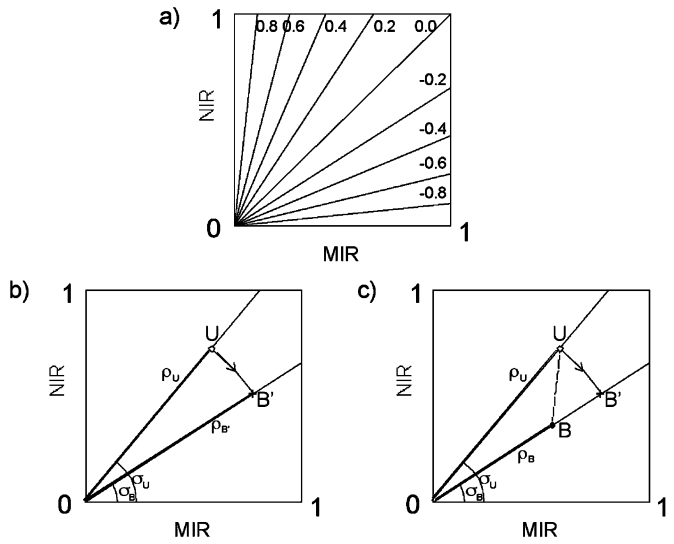

Fig. 1. (a) Isolines of the NBR index in near-infrared NIR and MIR spectral feature space. (b) Arc shows the ideal trajectory of changes in NIR and MIR reflectance from prefire (U) to ideal postfire (B') reflectance that is perpendicular to all NBR isolines. (c) |BB'| is the distance between the measured (B) and ideal (B') postfire reflectance along the NBR isoline of B; it is a measure of the spectral changes to which NBR is insensitive.

spatial resolutions. It explores how well NBR meets ideal requirements as an index sensitive to fire severity.

II. NBR for Quantifying Fire Severity

A. Theoretical Considerations

The NBR is defined from NIR and MIR reflectance as

$$\text{NBR} = \frac{\rho_{\text{NIR}} - \rho_{\text{MIR}}}{\rho_{\text{NIR}} + \rho_{\text{MIR}}}, \qquad -1 \leq \text{NBR} \leq 1. \tag{1}$$

In the spectral feature space of this index, all points of equal index value (isolines) fall along straight lines passing through the origin. This is illustrated in Fig. 1(a).

The multitemporal NBR difference

$$\Delta\text{NBR} = \text{NBR}_{\text{prefire}} - \text{NBR}_{\text{postfire}} \tag{2}$$

has been assumed to be directly proportional to fire severity and widely used to map fire severity [2], [9]–[11].

Ideally, if a spectral index is appropriate to the physical change of interest, then there is a simple relationship between the change and the direction of the displacement in spectral feature space [14]. The definition of an optimal spectral index requires that the trajectory in spectral feature space—in this case, arising from different levels of fire severity—is perpendicular to the index isolines [14]. Fig. 1(b) illustrates for NBR the optimal trajectory of a pixel from unburned (U) to burned (B') and the NBR index isolines that pass through these values (straight lines). In this figure ΔNBR is NBR(U) − NBR(B'). If the NBR index is optimal for describing fire severity, then burning should displace the NIR and MIR values along an arc of circumference joining (U) and (B').

In practice, factors introduced by the remote sensing and other processes perturb measured reflectance and are usually considered as noise. Such perturbing factors include atmospheric contaminations, bidirectional reflectance variations, changes in the sensed observation dimensions, and spectral variation at the surface unrelated to the parameter of interest. The reality of perturbing noise means a spectral index will usually not be optimal for describing a particular physical change of interest. This is illustrated in Fig. 1(c), which shows a measured burned pixel value (B) that does not fall on the arc of circumference passing through the unburned value (U), i.e., B ≠ B'.

In order to measure how NBR conforms to an optimal spectral index it is convenient to use polar coordinates (ρ, σ) [Fig. 1(b) and (c)]. For NBR, the condition of optimality is respected only if $\rho_{\text{U}} = \rho_{\text{B}}$. For unburned (U= $(\rho_{\text{U}}, \sigma_{\text{U}})$) and burned (B= $(\rho_{\text{B}}, \sigma_{\text{B}})$) values the corresponding ideal burned value (B' = $(\rho_{\text{U}}, \sigma_{\text{B}})$) falls by definition on the same NBR isoline as (B). Thus, the Euclidean distance |BB'| is related only to spectral changes to which NBR is insensitive, and so can be used as a measure of the optimality of ΔNBR. Observing that |UB| ≥ |BB'|, a normalized measure of optimality can be defined as

$$\Delta\text{NBR optimality} = 1 - \frac{|\text{BB'}|}{|\text{UB}|}, \qquad 0 \leq \Delta\text{NBR optimality} \leq 1. \tag{3}$$

The measure (3) allows us to assess the optimality of NBR, i.e., the degree that burning causes spectral displacements in the sensitivity direction of the NBR index. In the case of an optimal behavior of the index, changes from prefire (U) to postfire (B) are perpendicular to the index isolines and ΔNBR optimality = 1, as B ≡ B', and |BB'| = 0. Conversely, if the index is insensitive to changes due to burning, then all spectral changes occur along the index isolines and ΔNBR optimality = 0, as B'≡U, and |BB'| = |UB|.

Below, we first illustrate the methodology to assess ΔNBR optimality; that is the extent that the direction of displacements in the NIR-MIR space in relation to the NBR's isolines conform to the requirements of an index that is sensitive to fire severity. We then assess ΔNBR optimality using a number of remotely sensed data sets that capture a variety of fire severities and perturbing factors introduced by their remote sensing.

B. Illustration of the Method—Assessing NBR for Optimality Using in Situ Reflectance Data

We first illustrate the method to investigate NBR's optimality using *in situ* reflectance measurements made with a GER3700 spectroradiometer over savanna vegetation in Namibia [16]. All measurements were taken at 10.30 UTC, so bidirectional reflectance variations present in these data [17] are minimal.

Fig. 2 (left column) illustrates 19 reflectance measurements of adjacent unburned (open circles) and burned (solid circles) grass sites (top row), and similarly of adjacent unburned and burned shrub sites (bottom row). These measurements are plotted in the MIR-NIR spectral feature space used by NBR.

The data illustrated in Fig. 2 were chosen to incorporate different levels of fire severity. The prefire grass cover was homogeneous but burned with different behavior to deposit different amounts of char and white ash, reveal different amounts of litter and highly reflective Kalahari sand, and combust different amounts of grass. The prefire shrub cover was less homogenous than at the grass sites and also burned

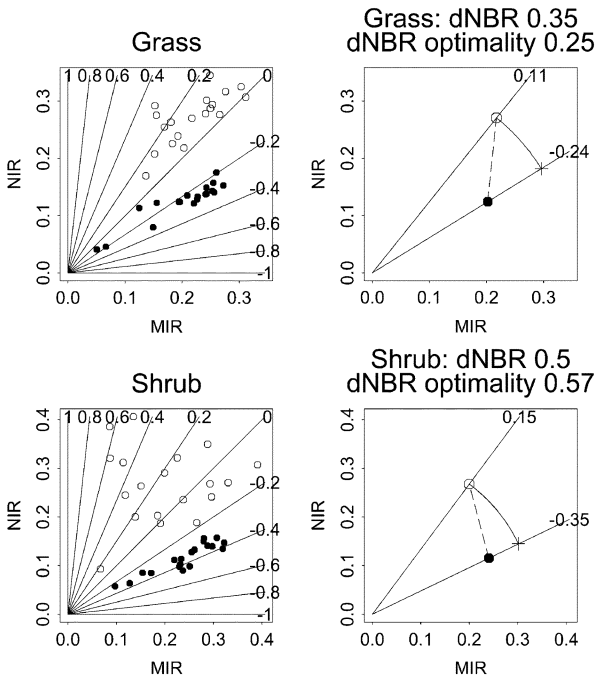

Fig. 2. (Left) Nineteen *in situ* NIR (858 nm) and MIR (2130 nm) reflectance measurements of savanna vegetation in Namibia (open circles = prefire, solid circles = postfire). NBR isolines and values are superimposed. (Right) Mean reflectance values with arcs to show the ideal reflectance trajectory from prefire to postfire values (crosses) if the NBR was optimal.

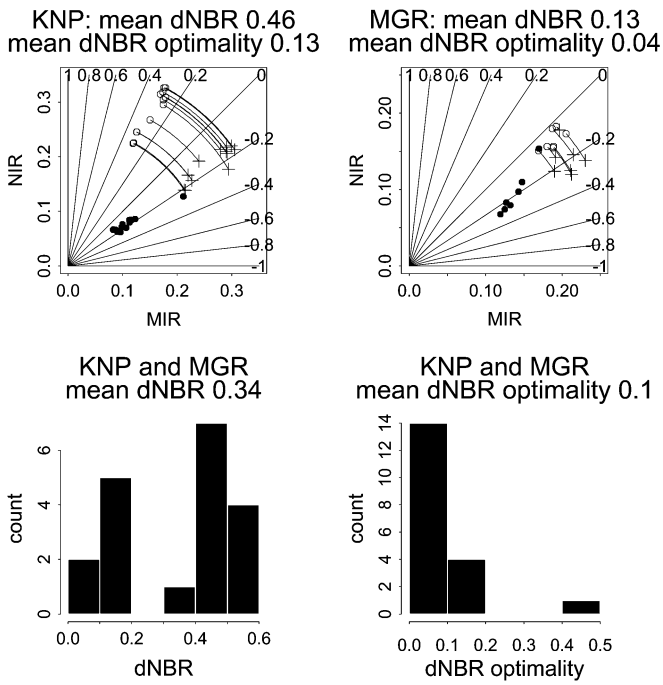

Fig. 3. (Top) Mean Landsat ETM+ NIR band 4 (750–900 nm) and MIR band 7 (2090–2350 nm) surface reflectance over 120 × 120 m sites before prescribed fires (open circles) and after prescribed fires (closed circles) at 12 sites in the Kruger National Park (KNP) and at seven sites in the Madikwe Game Reserve (MGR). The arcs show the ideal reflectance trajectory from prefire (open circles) to ideal postfire values (crosses) if the NBR was optimal. (Bottom) Histograms of ΔNBR and ΔNBR optimality for these 19 sites. The figure titles describe the mean ΔNBR and the mean ΔNBR optimality for the illustrated data.

differentially—with combustion of all leafy vegetation to reveal charred stems to only moderate shrub singeing.

The right column of Fig. 2 illustrates the averages of the unburned and burned reflectance values plotted with the NBR isolines that intersect them. It is evident that burning reduced average NBR, primarily by reducing the average NIR value and causing small changes in the average MIR value (reduced grass MIR and increased shrub MIR). The right column of Fig. 2 illustrates how pre- and postfire reflectance data from both sites are used to assess NBR for optimality. In particular, it shows the difference between the burned reflectance (solid circle) and the reflectance value predicted if the NBR was optimal (cross). The ΔNBR optimality values for these average changes are 0.25 for grass and 0.57 for shrub. Comparing these values with the optimal ΔNBR optimality value of 1 indicates that NBR is not optimal for these data.

Caution is needed in the interpretation of these illustrative results as the average prefire values at different locations are compared with average postfire values; this means that in Fig. 2 it is not possible to assess the displacement vector that connects any particular preburn location to its postburn equivalent. In the following sections, rather than compare average values over different locations, we more correctly compare data at the same pre- and postfire locations.

C. Assessing NBR Optimality Using Landsat ETM+ data

Fig. 3 (top row) illustrates atmospherically corrected Landsat ETM+ reflectance sensed before and after 19 prescribed surface fires lit in the south African dry season within Kruger National Park (KNP), and approximately 900 km west in the Madikwe Game Reserve (MGR), South Africa [3]. The Landsat ETM+ data were acquired within eight days of the different prescribed fires except for six of the prefire KNP Landsat data, which were acquired two months before the fires due to persistent cloud cover.

Fig. 3 illustrates data from 19 fires (12 in KNP and seven in MGR) lit on 120 × 120 m savanna sites with approximately homogenous vegetation structure and composition and less than 50% tree cover [3]. Prior to the fires, the MGR vegetation was seasonally more senescent (5% to 15% green) than at KNP (10% to 60% green), with slightly more exposed soil surfaces (approximately 5% to 10% surface area), less standing grass, and a higher shrub density. All the fires consumed the majority of the litter and much of the grass, shrub and tree canopy material below approximately 2 m. Field measurements were undertaken to estimate the site-level combustion completeness (cc) and the areal proportion that burned (f) by comparison of prefire and postfire fuel load measurements and postfire quadrat survey respectively [3]. At the KNP sites cc varied from 0.06–1.0 and f varied from 0.48–0.84, the MGR sites encompassed cc variation from 0.39–0.83 and f varied from 0.35–0.80 [3]. Therefore, the data are expected to encompass different levels of fire severity.

The reduction in ETM+ NIR reflectance caused by burning, evident in Fig. 3, was found to be positively related to cc and f [3]. NIR reflectance decreased more at the KNP than the MGR sites because the unburned reflectance values were higher at KNP than MGR and not because the KNP sites had higher values of cc and f [3]. Fig. 3 (bottom row) shows histograms of the 19 ΔNBR and ΔNBR optimality values for both sites.

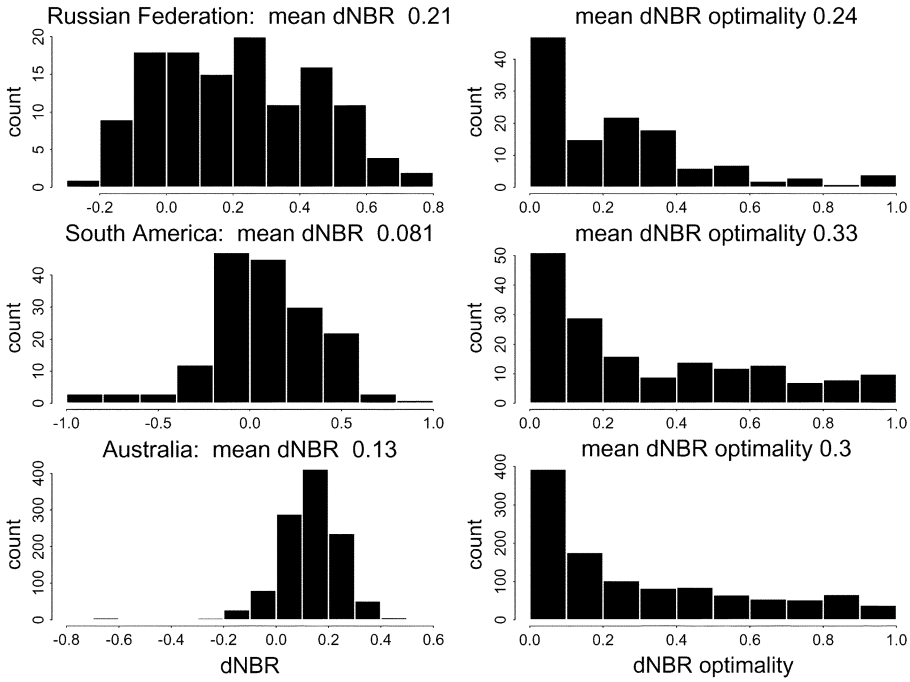

Fig. 4. Histograms of ΔNBR and ΔNBR optimality values computed from burned and unburned 500-m MODIS band 2 (858 nm) and band 7 (2130 nm) land surface reflectance values distributed across study regions in (top tow) the Russian Federation (125 pixels), (middle row) South America (169 pixels), and (bottom row) Australia (1120 pixels). Only MODIS observations sensed with a view zenith less than or equal to 20° are used.

The mean ΔNBR optimality value is 0.1 summarized over all sites, and is 0.13 and 0.04 for the KNP and MGR sites respectively. These low values indicate that the NBR is suboptimal for these nonforest data. We note that for other nonforest covers, [10] found poor correspondence between field-derived fire severity and ΔNBR (correlations 0.02–0.5); although [10] also found low correspondence for mixed forest (correlation 0.1) and closed needleleaf forest (correlation 0.38).

D. Assessing NBR Optimality Using MODIS Data

Another assessment of NBR optimality uses MODIS 500-m data. Fig. 4 shows histograms of MODIS 500-m ΔNBR and ΔNBR optimality values for observations sensed in predominantly boreal forest (Russian Federation), tropical forest (South America), and Savanna (Australia) study regions defined in [1]. These data were derived by examining the MODIS 500-m NIR and MIR land surface reflectance bands [18] at locations where 1-km MODIS active fires [19] were detected, following the methodology used to examine MODIS band burned-unburned separability described in [1] and [20]. This methodology is based on MODIS land surface reflectance observations and considers only observations that meet the following conditions: noncloudy, good quality, low, or average aerosol[1] sensed within ten days before or after a MODIS active fire detection. Observations sensed with a view zenith greater than 20° were not used; this served to reduce bidirectional reflectance variations and changes in the observation dimension (projected instantaneous field of view) that increase with MODIS view zenith angle [20]. Pre- and postfire reflectance values were selected from the observations occurring most closely before and after the active fire detections.

The data for the very different fire regimes illustrated in Fig. 4 are likely to encompass a range of fire severities. Because of the strict temporal constraint on the observations and the constraints placed on cloud cover, aerosol, and viewing geometry, it is possible to assume that the spectral changes are predominantly related to the different burning conditions, rather than to the effects of perturbing noise. For the same reasons, unburned proportions of postfire observations should be spectrally similar to the preburn proportions, with little expected impact on the NBR analysis.

Fig. 4 shows data for fires at 125 MODIS 500-m pixel locations in the Russian Federation, 169 in South America, and 1120 in Australia. The NBR values are smaller than observed in the Landsat ETM+ data as many of the fires detected by the 1 km MODIS active fire algorithm are smaller than the 1 km MODIS observation [19] and so changes in reflectance due to fire effects are likely to be smaller. As before the ΔNBR optimality values are low (means values of 0.24, 0.3, and 0.33) and the histograms show that the majority of values are close to 0, i.e., suboptimal.

III. Conclusion

Our findings using 30-m Landsat data sensed over the South African savanna and 500-m MODIS data sensed over Australian savanna, Russian Federation boreal forest, and South American tropical forest covers, do not provide evidence that the performance of the NBR is optimal in describing fire severity shortly after fire occurrence. For many of our results the NBR is far from optimal—with the NBR insensitive to changes due to burning, as most spectral change in the near-infrared and middle-infrared reflectance occurs nearly parallel to the NBR

[1]MODIS Land Surface Reflectance User's Guide: http://modis-sr.ltdri.org/html/guide.htm.

isolines. This may be a deterrent to the utility of the NBR index for certain applications.

As a future research topic, building an improved severity index should incorporate improved knowledge of how fires of different severity displace the position of prefire vegetation in multispectral space. This should also consider the uncertainties in the reflectance data resulting from the remote sensing acquisition and data preprocessing. This may allow not only the design of an index whose isolines are oriented to give the desired degree of sensitivity to fire severity while providing insensitivity to other possible sources of spectral variation; it could also allow a rigorous choice of the wavebands used.

One goal in the remote mapping of severity is to create a reliable method that allows it to be measured at different sites. This may be problematic however because of reflectance variability with respect to the numerous factors that may influence fire severity; given this variability it may not be possible to design an index that conforms closely to index theory and that works at different sites.

REFERENCES

[1] D. P. Roy, Y. Jin, P. E. Lewis, and C. O. Justice, "Prototyping a global algorithm for systematic fire-affected area mapping using MODIS time series data," *Remote Sens. Environ.*, vol. 97, pp. 137–162, 2005.

[2] C. H. Key and N. C. Benson, "Landscape assessment: Remote sensing of severity, the normalized burn ratio; and ground measure of severity, the composite burn index," in *FIREMON: Fire Effects Monitoring and Inventory System*, D. C. Lutes, R. E. Keane, J. F. Caratti, C. H. Key, N. C. Benson, and L. J. Gangi, Eds. Ogden, UT: USDA Forest Service, Rocky Mountain Res. Station, 2005, to be published.

[3] D. Roy and T. Landmann, "Characterizing the surface heterogeneity of fire effects using multitemporal reflective wavelength data," *Int. J Remote Sens.*, to be published.

[4] S. Tanaka, H. Kimura, and Y. Suga, "Preparation of a 1:25 000 Landsat map for assessment of burnt area on Etaijima Island," *Int. J. Remote Sens.*, vol. 4, pp. 17–31, 1993.

[5] K. C. Ryan and N. V. Noste, "Evaluating prescribed fires," in *Proc. Workshop on Wilderness Fire*. Ogden, UT, 1985, USDA Forest Service General Tech. Rep. INT-182, pp. 230–238.

[6] M. E. Jakubauskas, K. P. Lulla, and P. W. Mausel, "Assessment of vegetation change in a fire-altered forest landscape," *Photogramm. Eng. Remote Sens.*, vol. 56, no. 3, pp. 371–377, 1990.

[7] J. White, K. Ryan, C. Key, and S. Running, "Remote sensing of fire severity and vegetation recovery," *Int. J. Wildland Fire*, vol. 6, pp. 125–136, 1996.

[8] J. L. Michalek, J. E. Colwell, N. H. F. French, E. S. Kasischke, and R. D. Johnson, "Using Landsat TM data to estimate carbon release from burned biomass in an Alaskan spruce forest complex," *Int. J. Remote Sens.*, vol. 21, pp. 329–343, 2000.

[9] J. W. van Wagtendonk, R. R. Root, and C. H. Key, "Comparison of AVIRIS and Landsat ETM+ detection capabilities for burn severity," *Remote Sens. Environ.*, vol. 92, no. 3, pp. 397–408, 2004.

[10] J. Epting, D. Verbyla, and B. Sorbel, "Evaluation of remotely sensed indexes for assessing burn severity in interior Alaska using Landsat TM and ETM+," *Remote Sens. Environ.*, vol. 97, no. 1, pp. 92–115, 2005.

[11] A. E. Cocke, P. Z. Fule, and J. E. Crouse, "Comparison of burn severity assessments using differenced normalized burn ratio and ground data," *Int. J. Wildland Fire*, vol. 14, no. 2, pp. 189–198, 2005.

[12] J. Rogan and S. R. Yool, "Mapping fire-induced vegetation depletion in the peloncillo mountains, Arizona and New Mexico," *Int. J. Remote Sens.*, vol. 22, pp. 3101–3121, 2001.

[13] M. J. Lopez Garcia and V. Caselles, "Mapping burns and natural reforestation using Thematic Mapper data," *Geocarto Int.*, vol. 1, pp. 31–37, 1991.

[14] M. M. Verstraete and B. Pinty, "Designing optimal spectral indexes for remote sensing applications," *IEEE Trans. Geosci. Remote Sens.*, vol. 34, no. 5, pp. 1254–1265, Sep. 1996.

[15] M. M. Verstraete, B. Pinty, and R. B. Myneni, "Potential and limitations of information extraction on the terrestrial biosphere from satellite remote sensing," *Remote Sens. Environ.*, vol. 58, pp. 201–214, 1996.

[16] S. Trigg and S. Flasse, "Characterizing the spectral-temporal response of burned savannah using *in situ* spectroradiometry and infrared thermometry," *Int. J. Remote Sens.*, vol. 21, pp. 3161–3168, 2000.

[17] S. N. Trigg, D. P. Roy, and S. P. Flasse, "An *in situ* study of the effects of surface anisotropy on the remote sensing of burned savannah," Int. J. Remote Sens., to be published.

[18] E. F. Vermote, N. Z. El Saleous, and C. O. Justice, "Atmospheric correction of the MODIS data in the visible to middle infrared: First results," *Remote Sens. Environ.*, vol. 83, pp. 97–111, 2002.

[19] L. Giglio, J. Descloitres, C. O. Justice, and Y. J. Kaufman, "An enhanced contextual fire detection algorithm for MODIS," *Remote Sens. Environ.*, vol. 87, pp. 273–382, 2003.

[20] D. Roy, P. Lewis, and C. Justice, "Burned area mapping using multitemporal moderate spatial resolution data—A bi-directional reflectance model-based expectation approach," *Remote Sens. Environ.*, vol. 83, pp. 263–286, 2002.